Proteolytic Activation of Recombinant Pro-memapsin 2 (Pro-β-secretase) Studied with New Fluorogenic Substrates†

Jacques Ermolieff,‡ Jeffrey A. Loy,‡,§ Gerald Koelsch,‡ and Jordan Tang*,‡,§

Protein Studies Program, Oklahoma Medical Research Foundation, Oklahoma City, Oklahoma 73104, and Department of Biochemistry and Molecular Biology, University of Oklahoma Health Science Center, Oklahoma City, Oklahoma 73104

Received June 29, 2000

ABSTRACT: Memapsin 2 (β-secretase), a membrane-anchored aspartic protease, is involved in the cleavage of β-amyloid precursor protein to form β-amyloid peptide. The primary structure of memapsin 2 suggests that it is synthesized in vivo as pro-memapsin 2 and converted to memapsin 2 by an activating protease [Lin et al. (2000) *Proc. Natl. Acad. Sci. U.S.A. 97*, 1456−1460]. To simulate this activation mechanism and to produce stable mature memapsin 2 for kinetic/specificity studies, we have investigated the activation of recombinant pro-memapsin 2 by several proteases with trypsin-like specificity. Clostripain, kallikrein, and trypsin increased the activity of pro-memapsin 2. Clostripain activation was accompanied by the cleavage of the pro region to form mainly two activation products, Leu^{30p}- and Gly^{45p}-memapsin 2. Another activation product, Leu^{28p}-memapsin 2, was also purified. Kinetics of the activated memapsin 2 were compared with pro-memapsin 2 using two new fluorogenic substrates, Arg-Glu(5-[(2-aminoethyl)amino]-naphthalene-1-sulfonic acid (EDANS))-Glu-Val-Asn-Leu-Asp-Ala-Glu-Phe-Lys(4-(4-dimethylaminophenylazo)benzoic acid (DABCYL))-Arg and (7-methoxycoumarin-4-yl)acetyl (MCA))-Ser-Glu-Val-Asn-Leu-Asp-Ala-Glu-Phe-Lys(2,4-dinitrophenyl (DNP)). These results establish that the activity of pro-memapsin 2 stems from a part-time and reversible uncovering of its active site by its pro region. Proteolytic removal of part of the pro-peptide at Leu^{28p} or Gly^{45p}, which diminishes the affinity of the shortened pro-peptide to the active site, results in activated memapsin 2. These results also suggest that Glu^{33p}-memapsin 2 observed in the cells expressing this enzyme [Vassar et al. (1999) *Science 286*, 735−741; Yan et al. (1999) *Nature 402*, 533−537] is an active intermediate of in vivo activation, or that the peptide Glu^{33p}−Arg^{44p} may serve a regulatory role.

The deposit of the β-amyloid peptide (Aβ)[1] in the brain is generally regarded as a key event in the early pathogenesis of Alzheimer's disease (AD) (*1*). The 42/40-residue Aβ peptide, a major constituent of the senile plaques in AD brains, is derived from the proteolysis of a transmembrane protein, amyloid precursor protein (APP), by two proteases known as β-secretase and γ-secretase. The latter cleaves APP within the transmembrane domain and has been suggested to be another membrane protein, presenilin 1 (*2*). The β-secretase processing site is located in the region of APP accessible from the lumenal side of the membrane. Since the hydrolysis of this site is the rate-limiting step in the Aβ production in vivo (*3*), the responsible protease is considered to be the primary target for the design of inhibitor drugs against AD. The fact that the Swedish mutation of APP, in which the two amino acids at the amino-terminal side of the β-secretase cleavage site are changed from Lys-Met to Asn-Leu, results in an early onset of the disease (*4*) reinforces the idea that this protease is intimately involved in the pathogenesis of AD. The inhibition of β-secretase cleavage of APP in cultured cells by bafilomycin (*5*), an inhibitor for the lysosomal/endosomal hydrogen ion pump, suggests that this protease functions within acidic subcellular vesicles.

Recently, our group (*6*) and others (*7*−*10*) independently cloned a human brain aspartic protease, which we named memapsin 2, and showed it to be the long sought β-secretase. Memapsin 2 cDNA encodes for a prepro-protease, which shares strong sequence similarity and important structural motifs with other mammalian aspartic protease zymogens. Based on sequence aligment, memapsin 2 structure is extended at the C-terminus for about 80 residues, which includes a connecting strand to a single transmembrane strand and a short cytosolic region. The recombinant proteolytic unit of the pro-memapsin 2 is catalytically active, suggesting that it is an independently folding domain. Preliminary kinetic/specificity studies have also been reported (*6*). Although recombinant pro-memapsin 2 hydrolyzes peptide substrates at pH 4.0, it does not autocatalytically cleave within its pro region (Figure 1). In contrast, autocatalytic pepsinogen activation results in the removal of the entire pro-peptide (*11*). Memapsin 2 expressed in mammalian cells, however,

† G.K. is a Scientist Development Awardee of the American Heart Association (9930115N). J.T. is holder of the J.G. Puterbaugh Chair in Biomedical Research at the Oklahoma Medical Research Foundation.

* To whom correspondence should be addressed. Phone: (405) 271-7291. Fax: (405) 271-7249. E-mail: jordan-tang@omrf.ouhsc.edu.

‡ Oklahoma Medical Research Foundation.

§ University of Oklahoma Health Science Center.

[1] Abbreviations: Aβ, β-amyloid peptide; APP, β-amyloid precursor protein; AD, Alzheimer's disease; EDANS, 5-[(2-aminoethyl)amino]-naphthalene-1-sulfonic acid; DABCYL, 4-(4-dimethylaminophenylazo)-benzoic acid; MCA, (7-methoxycoumarin-4-yl)acetyl; DNP, 2,4-dinitrophenyl; Nph, *p*-nitrophenylalanine; DMSO, dimethyl sufoxide.

10.1021/bi001494f CCC: $19.00
Published on Web 09/13/2000

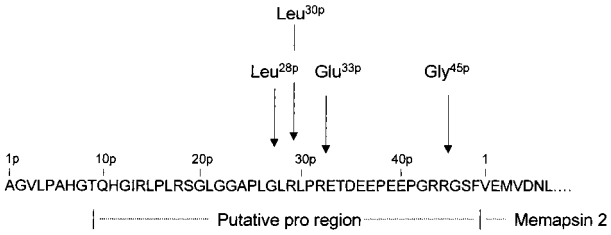

FIGURE 1: Amino acid sequences of the pre, pro, and N-terminal regions of human memapsin 2. Residues 1p−47p are present in recombinant pro-memapsin 2. The putative pro region, residues 9p−47p, is based on homology sequence alignment with the pro region of human pepsinogen. The positions of starting residues for different memapsin 2 species are indicated by vertical arrows.

is derived from the cleavage of its pro-enzyme at an Arg^{32p}−Glu^{33p} bond (*7*, *8*,) and is longer than its aligned N-terminal position by 16 residues. In addition, located at only 5−6 residues away from its aligned N-terminal position is an Arg^{43p}−Arg^{44p} sequence (Figure 1), which is a well-known motif for posttranslational processing (*12*, *13*), including the activation cleavage of pro-renin. These observations suggest that the activation of pro-memapsin 2 in vivo is likely mediated by another protease. We have therefore studied in vitro activation of recombinant pro-memapsin 2 by several proteases. New sensitive fluorogenic substrates have also been developed for these studies. Here we report that cleavage of the pro-peptide from pro-memapsin 2 by other proteases results in the activation of the enzyme.

EXPERIMENTAL PROCEDURES

Materials

Memapsin 2 inhibitor OM99-2 was synthesized as previously described (*14*). Fluorogenic substrate FS-1, NH_2-Arg-Glu(EDANS)-Glu-Val-Asn-Leu-Asp-Ala-Glu-Phe-Lys(DABCYL)-Arg-COOH, was synthesized at SynPep (Dublin, CA). Fluorogenic substrate FS-2, (MCA)Ser-Glu-Val-Asn-Leu-Asp-Ala-Glu-Phe-Lys(DNP), and chromogenic substrate Glu-Val-Asn-Nph-Asp-Ala-Glu-Phe (Nph = *p*-nitrophenylalanine) were synthesized at the Molecular Biology Resource Center, University of Oklahoma Health Sciences Center, using an Applied Biosystems Peptide synthesizer 430A. Bovine trypsin, clostripain from *Clostridium histolyticum*, human plasma kallikrein, and murine tissue kallikrein were purchased from Sigma. Human furin and murine proprotein convertase 1 were purchased from ALEXIS Biochemical (Switzerland). Factor Xa was purchased from Haematologic Technologies Inc. (Essex Junction, VT). Other reagents were the highest grade commercially available.

Methods

Preparation of the Protease Domain of Leu^{28p}- and Pro-memapsin 2. The recombinant protease unit of pro-memapsin 2 (pro-memapsin 2_{pd}) was prepared from *E. coli* expression as inclusion bodies, refolded, and purified as previously described (*6*). In the construct, the current recombinant pro-memapsin 2_{pd} sequence starts at residue Ala^{1p} (Figure 1) and ends at residue Thr^{367} (*6*). For the convenience of discussion, pro-memapsin 2_{pd} will be referred to as pro-memapsin 2, and the activated memapsin 2_{pd} will be referred to as memapsin 2 throughout this paper. The three memapsin 2 species discussed below have different cleavage points in the putative pro region, and their N-terminal positions are indicated by their respective starting amino acids and residue numbers. Leu^{28p}-memapsin 2, an activated form of memapsin 2, was formed during the purification of pro-memapsin 2, possibly by an *E. coli* protease. Leu^{30p}-memapsin 2 and Gly^{45p}-memapsin 2 were produced from clostripain activation of pro-memapsin 2 (see below) and are discussed under Results.

Activation of Pro-memapsin 2 by Proteases. Pro-memapsin 2 was individually incubated with the following proteases: trypsin, clostripain, plasma and tissue kallikrein, factor Xa, furin, and proprotein convertase 1. The reaction was carried out at 37 °C, and aliquots were taken at various time points for kinetic studies. In a few cases, aliquots were also applied on a 10% Tricine SDS gel (Novex, San Diego). The gel bands produced from activation were transferred to a PVDF membrane and analyzed for the N-terminal sequences using automated Edman degradation. For preactivation, proprotein convertase 1 was incubated for 30 min in 0.1 M sodium acetate, 5 mM $CaCl_2$, 0.01% Triton X-100, pH 5.5, and clostripain (5.6 mg) was dissolved in 600 μL of 0.1 M Tris-HCl, 8 mM DTT, 20 mM $CaCl_2$ at pH 8.0 and left 1 h at 0 °C.

The incubation buffers for the activation of pro-memapsin 2 are as follows: for clostripain, 0.1 M Tris-HCl, 8 mM DTT, 20 mM $CaCl_2$, pH 8.0; for trypsin, 0.1 M Tris-HCl, 0.4 M urea, 0.2 M NaCl, pH 8.0; for furin, 0.1 M Hepes, 1 mM $CaCl_2$, 0.5% Triton X-100, 1 mM β-mercaptoethanol, pH 7.6; and for kallikreins and factor Xa, 0.1 M Hepes 0.1 M NaCl, 5 mM $CaCl_2$.

Isolation of Activated Memapsin 2. Pro-memapsin 2 was preincubated in the presence of clostripain for various lengths of time in order to produce the desired memapsin 2 species for purification. To isolate Leu^{30p}-memapsin 2, 26.7 μM pro-memapsin 2 was incubated with 62.0 nM clostripain at 37 °C for 5 min. To obtain Gly^{45p}-memapsin 2, 18.3 μM pro-memapsin 2 and 16.4 nM clostripain were incubated at 37 °C for 4−5 h. Proteolytically activated forms of memapsin 2 were purified using a 1 mL Resource S column on an FPLC apparatus (Pharmacia) equilibrated in a buffer of 0.1 M Tris-HCl, 0.4 M urea and eluted with a gradient of NaCl. Quantification of enzymes was achieved by active-site titration using a tight-binding inhibitor, OM99-2 (*14*).

Assay for Memapsin 2 Activity. Unless specified otherwise, all the kinetic experiments were performed in a buffer of 0.1 M sodium acetate, pH 4.5 at 37 °C, with 10% dimethyl sulfoxide (DMSO) using either substrate FS-1 or substrate FS-2 (Figure 2). The hydrolysis of substrates at the intended bonds was confirmed by analysis of the products in LC/MS (results not shown). The increase of fluorescence intensity produced during substrate hydrolysis was studied in a continuous assay using an AMINCO-Bowman Series 2 fluorescence spectrophotometer. An excitation wavelength of 350 nm and an emission wavelength of 490 nm were used to monitor the hydrolysis of substrate FS-1. For substrate FS-2, excitation at 328 nm and emission at 393 nm were used. In kinetic studies, the rates of substrate hydrolysis taken from the measurement of initial fluorescence change are directly proportional to the enzyme concentrations. Sodium acetate buffer, 0.1 M, was used for determination of activity

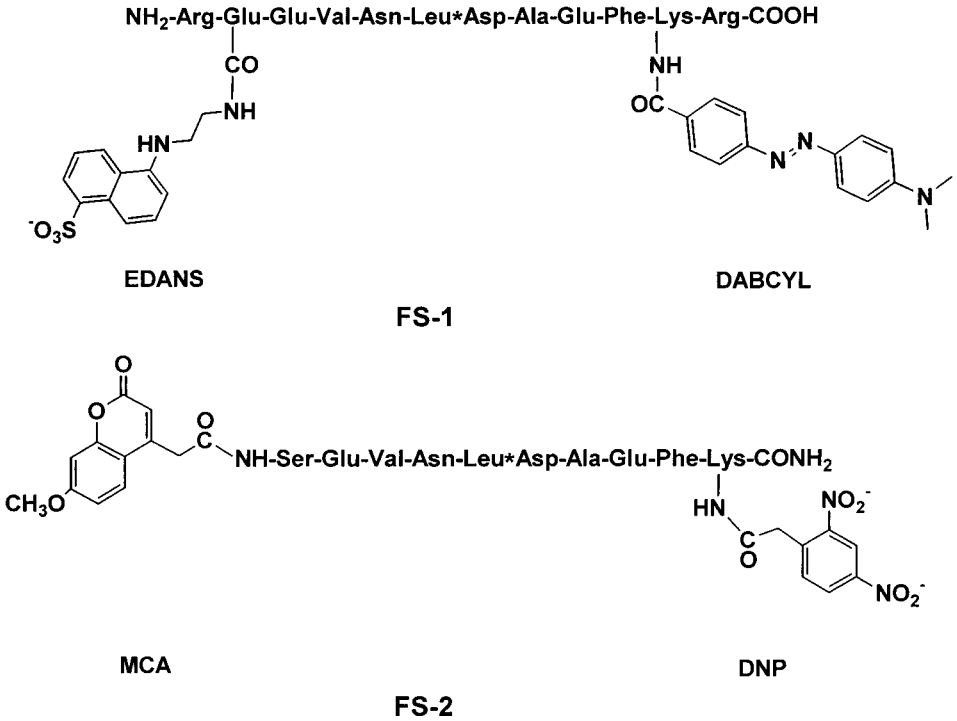

FIGURE 2: Structures of fluorogenic substrate 1 (FS-1) and fluorogenic substrate 2 (FS-2).

in pH range of 3.5−5.5. Citrate buffer, 0.1 M, was used for pH 3.0.

Determination of the Kinetic Constants, K_m and k_{cat}. Kinetic parameters, K_m and V_{max}, were obtained from the fitting of the data using nonlinear regression analysis software GraFit (*15*). The k_{cat} values (s^{-1}) were determined from the V_{max} values using the equation:

$$k_{cat} = \frac{V_{max}}{F/[S]_0[E]_0}$$

where F is the amplitude of fluorescence after complete substrate hydrolysis, V_{max} is the maximum rate of substrate hydrolysis determined in arbitrary units of fluorescence per second, $[S]_0$ is the initial concentration of fluorogenic substrate, and $[E]_0$ is the initial concentration of active memapsin 2 determined by active site titration using the tight-binding inhibitor OM99-2.

Determination of Inhibition Constants, K_i. The inhibition constants, K_i, against inhibitor OM99-2 were determined for pro-memapsin 2 and different memapsin 2 species as described by Bieth (*16*). The hydrolysis of the fluorogenic substrate FS-2, $[S]_0$, for a series of mixtures with constant enzyme, $[E]_0$, but increasing inhibitor concentration, $[I]_0$, was carried out as described above. The apparent inhibition constant, K_{iapp}, was determined from the plot of activity vs $[I]_0$ based on the equation:

$$a = 1 - \frac{[I]_0 + [E]_0 + K_{iapp} - \sqrt{([I]_0 + [E]_0 + K_{iapp})^2 - 4[I]_0[E]_0}}{2[E]_0}$$

The inhibition constant, K_i, was determined using substrate FS-2 from a series of K_{iapp} obtained from different substrate concentrations, ranging from 1.9 to 2.8 mM, since the K_i was found to be independent of substrate concentration. The K_i determined with FS-1 used the substrate concentration of 8.2 μM.

Measurement of Association and Dissociation Rate Constants for the Binding of OM99-2 to Memapsin 2. Association and dissociation of pro-memapsin 2 and memapsin 2 with inhibitor OM99-2 were followed by surface plasmon resonance using a BIAcore 1000 biosensor (BIAcore Inc.) in the OMRF BIAcore Core Facility. OM99-2 was immobilized onto the surface of a carboxylated dextran matrix (CM-5) sensor chip using the amine-coupling kit provided by the manufacturer and a flow rate of 5 μL/min with 100 μg/mL inhibitor solution in 90 mM Hepes, pH 7.4, containing 10% DMSO. After coupling, the sensor surface was blocked using 1 M ethanolamine, pH 8.5. Binding experiments were performed in a running buffer containing 10 mM sodium acetate, pH 4.5, 20 mM NaCl, and 0.005% surfactant P-20 at 25 °C using a flow rate of 30 μL/min. The concentrations of pro-memapsin 2 and memapsin 2 used were in the range of 5−140 nM. Association and dissociation rates, k_{on} and k_{off}, were determined over 80 and 100 s, respectively. The sensor was regenerated with 6 M guanidine hydrochloride followed by 100 mM triethylamine, pH 11.5. After subtraction of the nonspecific refractive index component, the kinetic constants were calculated from the sensorgrams by nonlinear fitting of the association and dissociation curves according to a simple bimolecular mechanism: A + B ⇄ AB, using BIAevaluation software version 3.0 (BIAcore, Sweden).

RESULTS

Synthetic Substrates for the Assay of Memapsin 2 Activity. To develop convenient assays for memapsin 2, we designed and tested two fluorogenic substrates and a chromogenic substrate. The fluorogenic substrates FS-1 and FS-2 (Figure 2) each contain the sequence of Glu-Val-Asn-Leu-Asp-Ala-

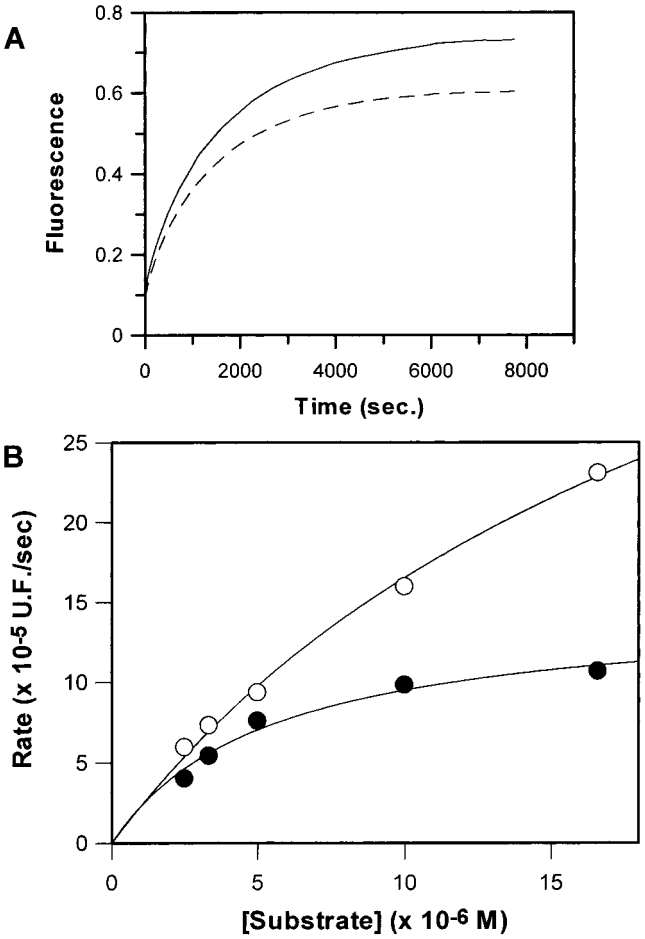

FIGURE 3: Increase in fluorescence during the hydrolysis of 6.2 and 5.1 μM FS-1 (A) and kinetic plot for the hydrolysis of fluorogenic substrate FS-1 in the presence of 0.37 μM Leu^{28p}-memapsin 2 (open circles) and pro-memapsin 2 (closed circles) (B). U.F. is arbitrary fluorescent unit.

Table 1: Kinetic Parameters of Pro-memapsin 2 and Its Proteolytically Activated Species

substrate	enzyme	K_m (μM)	k_{cat} (min^{-1})	k_{cat}/K_m (min$^{-1}/\mu$M)
FS-1	pro-memapsin 2	5.40 ± 1.10	0.24 ± 0.02	0.044 ± 0.005
	Leu^{28p}-memapsin 2	22.60 ± 4.10	0.90 ± 0.01	0.040 ± 0.007
FS-2	pro-memapsin 2	4.50 ± 1.40	0.25 ± 0.04	0.056 ± 0.008
	Leu^{28p}-memapsin 2	5.03 ± 1.72	0.40 ± 0.06	0.080 ± 0.015
	Gly^{45p}-memapsin 2	5.80 ± 1.99	0.94 ± 0.21	0.160 ± 0.019

Glu-Phe from the β-secretase site of the Swedish mutation of APP. We have previously shown that the hydrolysis of the Leu−Asp bond in the unmodified peptide with this sequence produced favorable kinetic parameters (*6*). The current substrates utilize the principle of resonance energy transfer (*17*, *18*) and contain EDANS and MCA as fluorophores and DABCYL and DNP as quenching groups, respectively. The hydrolysis of these substrates separates the fluorophores from the quenching groups, resulting in an increase of fluorescence (Figure 3A). Kinetic plots of one of these substrates are shown in Figure 3B. For recombinant pro-memapsin 2, the kinetic parameters at pH 4.5 are K_m = 5.4 μM and k_{cat} = 0.24 min^{-1} for FS-1 and K_m = 4.5 μM and k_{cat} = 0.25 min^{-1} for FS-2 (Table 1). Compared to the unmodified peptide substrate (*6*), both FS-1 and FS-2 have much lower K_m and k_{cat} values. During the course of this study, we have demonstrated that these substrates have high sensitivity and reproducibility and are also convenient to use for routine kinetic assays. On the other hand, the chromogenic substrate with a *p*-nitrophenylalanine group in the P_1 position proved to be a very poor substrate and not suited for kinetic assays. The kinetic constants of this substrate for pro-memapsin 2 are K_m = 0.13 ± 0.05 mM and k_{cat} = 1.58 ± 0.27 min^{-1}.

Proteolytic Activation of Pro-memapsin 2 and Isolation of Activation Products. Pro-memapsin 2 was incubated separately with proteases having specificity toward basic residues. We observed an increase of activity of up to 90% during the course of incubation with trypsin, clostripain, and kallikrein (Figure 4A,B). Furin, factor Xa, and proprotein convertase 1 were ineffective (results not shown). Trypsin increased pro-memapsin 2 activity only 40% at maximum and then declined thereafter (Figure 4A), indicating that it may also proteolytically inactivate memapsin 2 activity. Clostripain and the two kallikreins formed stable activity after reaching maximal activation. Aliquots taken at different times during the clostripain activation of pro-memapsin 2 and analyzed in SDS−PAGE showed a 48 kDa intermediate early in the time course (Figure 4C, 5−15 min) and then two stable activated forms of 46 and 44 kDa (Figure 4C, 20−30 min). The activation products from the longer incubation were isolated from FPLC separation (Figure 5). The N-terminal sequence of the isolated protein established that clostripain cleaved the pro sequence of memapsin 2 at Arg^{29p}−Leu^{30p} to produce the 46.1 kDa Leu^{30p}-memapsin 2 and at Arg^{44p}−Gly^{45p} to produce the 44.1 kDa Gly^{45p}-memapsin 2 (Figure 1). These results indicated that the increase of pro-memapsin 2 activity by clostripain was due to the cleavage and removal of part of the pro-peptide.

Kinetic Parameters of Leu^{28p}-, Gly^{45p}-, and Pro-memapsin 2. Although the k_{cat} value for Leu^{28p}-memapsin 2 is more than 3 times that for pro-memapsin 2 when determined with substrate FS-1, the K_m of Leu^{28p}-memapsin 2 is about 4 times higher (Table 1). This unfavorable K_m for Leu^{28p}-memapsin 2, which is not observed using substrate FS-2 (Table 1), prompted us to use only FS-2 for the rest of the studies. For this substrate, the K_m values of pro-memapsin 2 and the two activated memapsin 2 species are very close (Table 1). The ratios of k_{cat} values of pro-memapsin 2, Leu^{28p}-memapsin 2, and Gly^{45p}-memapsin 2 are about 1:2:4 (Table 1). Their k_{cat}/K_m values bear a similar relationship. The pH dependence of the activity of pro-memapsin 2, Leu^{28p}-memapsin 2, and Gly^{45p}-memapsin 2 shows the expected bell-shaped curves from pH 3.5 to 5.5 (Figure 6). The activity at pH 3.0 was, however, not measurable due to irreversible inactivation of the enzyme, which was demonstrated by preincubation at pH 3.0 and assay at a higher pH.

Inhibition of Leu^{28p}-, Gly^{45p}-, and Pro-memapsin 2 by OM99-2. OM99-2 is a designed transition-state inhibitor with a K_i of 9.8 × 10^{-9} M for pro-memapsin 2 (*14*). With the availability of activated memapsin 2 species, it is now possible to determine the K_i values for the activated enzyme. We determined the K_i of OM99-2 vs Leu^{28p}-memaspin 2 to be (1.4 ± 0.4) × 10^{-9} M using substrate FS-2 (Table 2). The K_i value for Gly^{45p}-memapsin 2 was found to be (1.5 ± 0.6) × 10^{-9} M using substrate FS-2. Since the assays were carried out in the presence of 10% DMSO, we also determined the inhibition of Leu^{28p}-memapsin 2 in 4% and

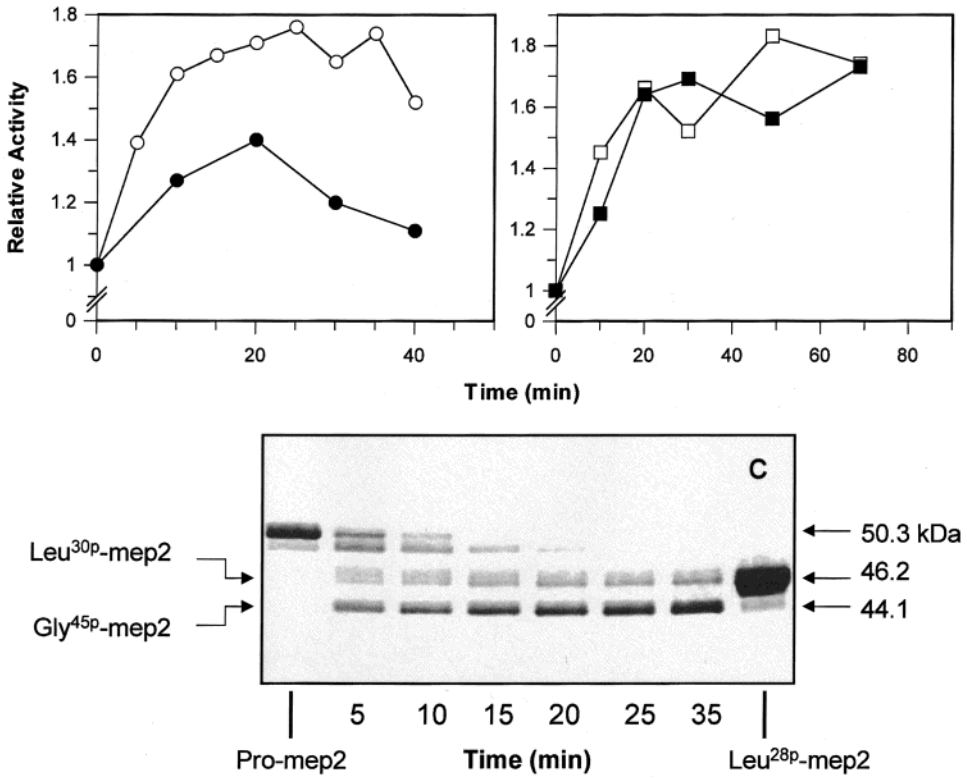

FIGURE 4: Increase of proteolytic activity during incubation of pro-memapsin 2 with proteases: (A) clostripain (open circles) and trypsin (closed circles); (B) human plasma kallikrein (open squares) and murine tissue kallikrein (closed squares). (C) SDS−polyacrylamide gel electrophoresis of aliquots taken at different incubation times from the activation of pro-memapsin 2 by clostripain.

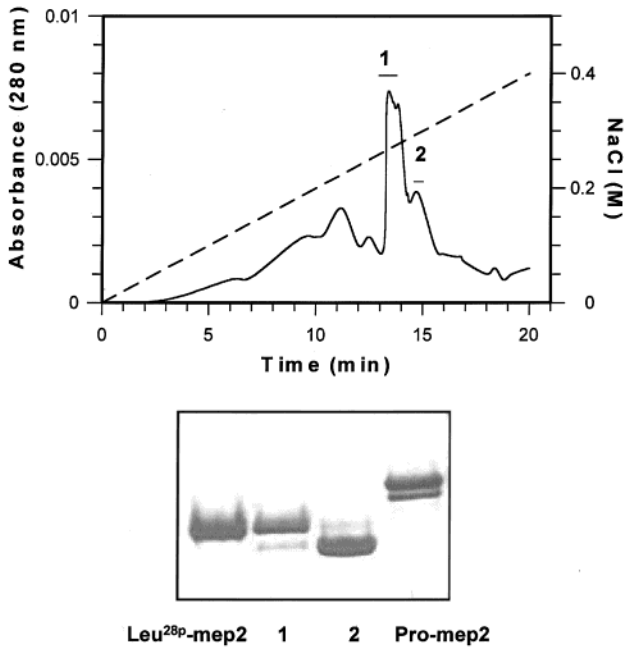

FIGURE 5: FPLC purification of Gly^{45p}-memapsin 2 species from the clostripain activation of pro-memapsin 2. Pro-memapsin 2 (18.3 μM) was incubated 4.5 h in the presence of clostripain (16.4 nM) at 37 °C. The material was applied on a 1 mL Resource S column equilibrated in 0.1 M Tris with 0.4 M urea, pH 6.0. The proteins were eluted with a gradient of NaCl (dashed line). A similar protocol was used to isolate Leu^{30p}-, Leu^{28p}-, and pro-memapsin 2 (not shown). The purity of the material eluted was determined by SDS−PAGE (bottom panel). Results show a single band for Leu^{30p}- (**1**), and Gly^{45p}-memapsin 2 (**2**).

15% DMSO using FS-1 and obtained the K_i values of (1.6 ± 0.5) × 10^{-9} M and (2.0 ± 1.0) × 10^{-9} M, respectively.

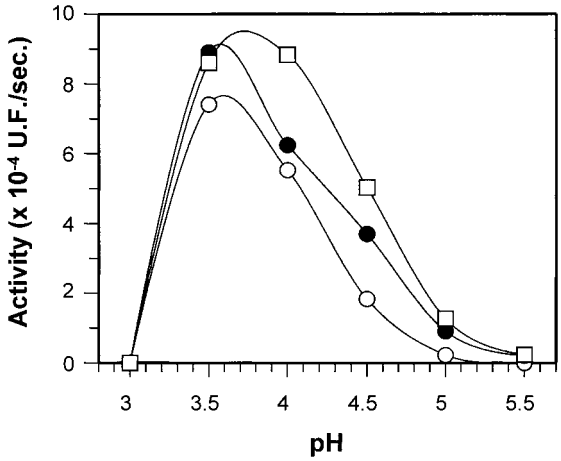

FIGURE 6: pH dependence of the hydrolytic activity of pro-memapsin 2 (open circles), Leu^{28p}-memapsin 2 (closed circles), and Gly^{45p}-memapsin 2 (squares).

Since these three values are within normal random errors of the method, the inhibition kinetics are not affected by up to 15% DMSO.

Binding of Pro-memapsin 2 and Leu^{28p}-memapsin 2 to OM99-2. The binding of pro-memapsin 2 and Leu^{28p}-memaspin 2 to OM99-2 was measured in a BIAcore instrument with OM99-2 covalently attached to the sensor chip. The sensograms representing the binding and dissociation of pro-memapsin 2 and memapsin 2 to inhibitor OM99-2 are shown in Figure 7, while the k_{on}, k_{off}, and equilibrium dissociation constants, K_d, are shown in Table 2. The two k_{off} values are very close; the k_{on} of memapsin 2 is 3 times that for pro-memapsin 2. The K_d values agree reasonably with the K_i values.

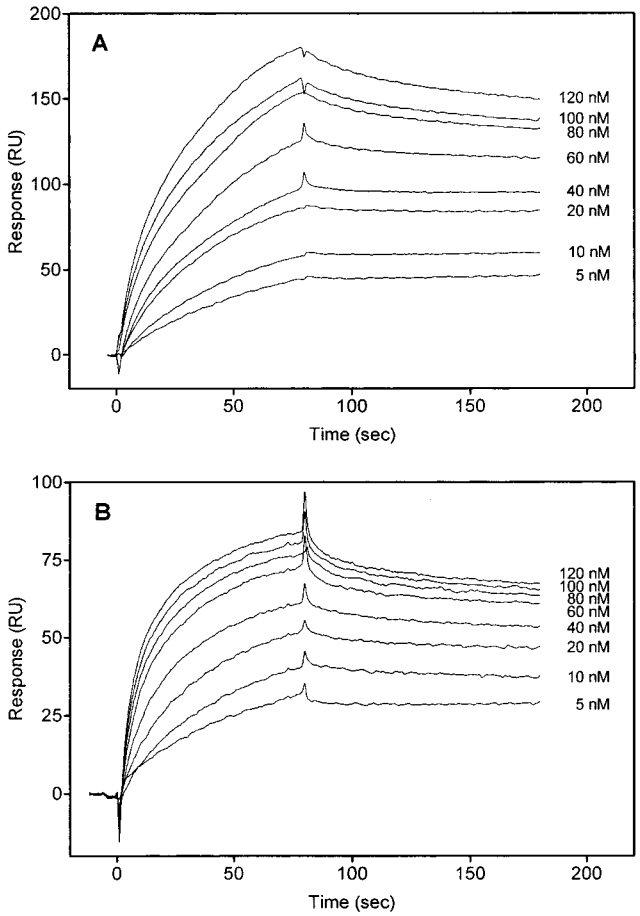

FIGURE 7: Sensorgram overlays for the binding and dissociation of inhibitor OM99-2 from pro-memapsin 2 (A) and Leu^{28p}-memapsin 2 (B).

Table 2: Kinetics of Pro-memapsin 2 and Leu^{28p}-memapsin 2 Binding to Inhibitor OM99-2

enzyme	k_{on} ($\times 10^5$ M^{-1} s^{-1})	k_{off} ($\times 10^{-3}$ s^{-1})	K_d (nM)	K_i (nM)
pro-memapsin 2	3.29 ± 0.04	1.17 ± 0.02	3.55 ± 0.02	9.8 [a]
Leu^{28p}-memapsin 2	10.3 ± 0.13	1.04 ± 0.02	1.01 ± 0.01	1.4 ± 0.4 [b]

[a] Ref *14*. [b] Average of K_i values (see Results).

DISCUSSION

Based on sequence alignment with other aspartic proteases, pro-memapsin 2 is predicted to start near residue Thr^{9p} and memapsin 2 may start near residue Val^{48p} (Figure 1). The sequence of recombinant pro-memapsin 2 includes residues 1p−48p; thus, it should contain the entire pro region. Yet, the recombinant pro-memapsin 2 is enzymically active (*6*). This activity is apparently that of the pro-enzyme since it does not autocatalytically cleave within the pro region, in opposition to the acid-triggered activation of many aspartic protease pro-enzymes (*19*). In the crystal structures of other mammalian aspartic protease zymogens, the pro-peptides block the entrance to the respective active-site clefts (*20*−*22*). The native conformation of the pro region in pro-memapsin 2 is expected to assume the same blockade of its active site. The catalytic activity of pro-memapsin 2, therefore, suggests that the conformation of its pro domain exists in two equilibrium forms: one with the active site 'open' and other with the active site 'closed' by virtue of a propeptide blockade (Figure 8). There are several examples

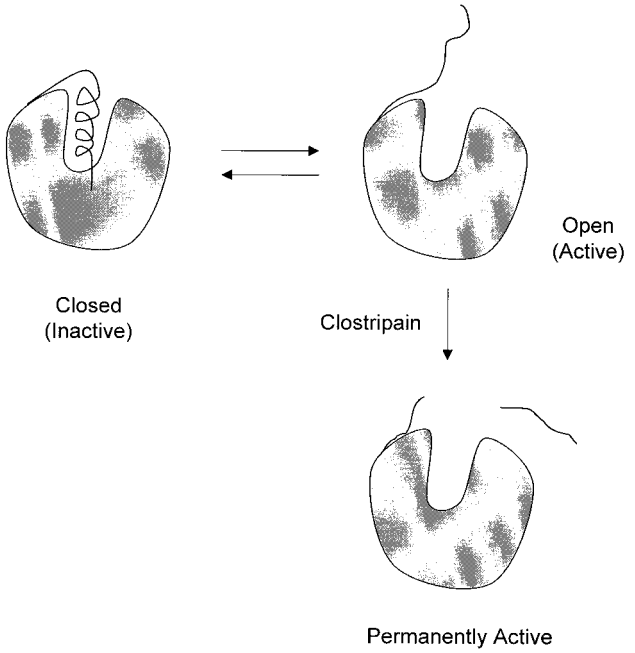

FIGURE 8: Schematic presentation of two conformational forms of pro-memapsin 2. In the 'closed' form, the pro-peptide assumes its native conformation and blocks the entrance of the active-site cleft. In the 'open' form, the pro region is not blocking the active-site cleft, and thus permits proteolysis or binding with inhibitor. The cleavage of pro-peptide at Gly^{27p}/Leu^{28p} or Arg^{44p}/Gly^{45p} produces memapsin 2 species with available active site.

of this phenomenon among aspartic protease zymogens. The initial exposure of the active site of pepsinogen in acidic solution is part of its activation mechanism (*19*). The structure of an activation intermediate of progastricsin with an exposed active site has been determined (*23*). Prorenin, which is thought to be activated by an Arg-Arg-specific protease, also reversibly uncovers its active site (*24*). While the 'opening' of the pepsinogen active site is triggered by hydrogen ion concentration (*19*), the equilibrium between the 'open' and 'closed' forms of pro-memapsin 2 at different pH does not appear to significantly change due to the loss of residues 1p−28p. This is demonstrated by the lack of a significant trend in the pH dependence of the ratios between activities of pro-memapsin 2 and Leu^{28p}-memapsin 2 (see Figure 6). The increase of activity from the incubation of pro-memapsin 2 with clostripain and other proteases must be a result of the removal of part of the pro-peptide, which reduces the affinity between the remaining pro segment and the catalytic unit, and thus results in exposing the active site to full-time catalysis (Figure 8). The higher k_{cat} and k_{cat}/K_m values of activated memapsin 2 over the pro-enzyme are consistent with this hypothesis.

The fact that Gly^{45p}-memapsin 2 has a higher activity than other activated species (Leu^{28p}- and Leu^{30p}-memapsin 2) suggests that it may be the final in vivo activation product derived from cleavage just beyond the Arg^{43p}-Arg^{44p} motif. Since the N-terminal positions of Leu^{30p}-memapsin 2 and Gly^{33p}-memapsin 2 are quite near, their activities are likely to be similar. In the in vitro activation experiments with clostripain, we did not observe cleavage of the Arg^{32p}−Glu^{33p} bond, which appears to be the predominant cleavage site in vivo (*7*, *8*). This difference suggests that the in vivo cleavage may be accomplished by a protease with specificity toward an Arg−Glu bond. It is possible that Glu^{33p}-memapsin 2 may

be an intermediate with a longer survival time in vivo cells. It is also possible that partial activation with the retention of a portion of the putative pro-peptide $Glu^{33p}-Arg^{44p}$ may have functions such as the modulation of memapsin 2 activity.

The catalytic activity of pro-memapsin 2 can be physiologically functional. Since the zymogen is catalytically active only below pH 5.5 (Figure 6), it is likely that its activity is not expressed until the zymogen reaches the site where it normally functions (*3*, *11*, *25*). The opening of the active site may provide instant activity and also make the pro-peptide more accessible to cleavage by an activating protease.

The presence of the 'open' and 'closed' forms of pro-memapsin 2 as suggested from the kinetic data was further confirmed by their difference in binding to inhibitor OM99-2 (Figure 7 and Table 2). The dissociation rate constants, k_{off}, for pro-memapsin 2 and Leu^{28p}-memapsin 2 are very close (Table 2), indicating that once bound, the two enzyme−inhibitor complexes are alike. The association rate constant, k_{on}, of Leu^{28p}-memapsin 2 is, however, 3 times that for pro-memapsin 2, indicating that only about one-third of pro-memapsin 2 molecules are in the 'open' conformation for inhibitor binding. The data also indicate that the rate of the transition from the 'closed' form to the 'open' form of pro-memapsin 2 is slower than the binding of inhibitor to its active site under the conditions of the BIAcore experiments. The equilibrium dissociation constants, K_d, calculated from the binding data agree well with the inhibition constants, K_i, measured by kinetic assays.

The kinetics and inhibition of memapsin 2 are basic tools to the development of new memapsin 2 inhibitors with pharmaceutical potentials. We have demonstrated here that recombinant pro-memapsin 2 can produce fully active memapsin 2 for such assays. Additionally, fluorogenic substrates developed were instrumental for generating the kinetic data in this study. From our experience, these fluorogenic assays for memapsin 2 are much more convenient than the HPLC-based assay we previously reported (*6*). The poor K_m of the chromogenic substrate, possibly from a poor fit of the *p*-nitrophenylalanine side chain in enzyme subsite P_1, renders it unsuitable as a tool for kinetic studies.

ACKNOWLEDGMENT

We thank Angela Irwin for the preparation of pro-memapsin 2, Dr. Ken Jackson of the Warren Medical Research Foundation, University of Oklahoma Health Sciences Center, for assisting in peptide synthesis, Dr. Pierre Neuenschwander for helpful discussions in BIAcore experiments, and Dr. Jean A. Hartsuck for constructive criticism of the manuscript.

REFERENCES

1. Selkoe, D. J. (1999) *Nature 399*, A23−31.
2. Wolfe, M. S., Xia, W., Ostaszewski, B. L., Diehl, T. S., Kimberly, W. T., and Selkoe, D. J. (1999) *Nature 398*, 513−517.
3. Sinha, S., and Lieberburg, I. (1999) *Proc. Natl. Acad. Sci. U.S.A. 96*, 11049−11053.
4. Mullan, M., Crawford, F., Axelman, K., Houlden, H., Lilius, L., Winblad, B., and Lannfelt, L. (1992) *Nat. Genet. 1*, 345−347.
5. Knops, J., Suomensaari, S., Lee, M., McConlogue, L., Seubert, P., and Sinha, S. (1995) *J. Biol. Chem. 270*, 2419−2422.
6. Lin, X., Koelsch, G., Wu, S., Downs, D., Dashti, A., and Tang, J. (2000) *Proc. Natl. Acad. Sci. U.S.A. 97*, 1456−1460.
7. Vassar, R., Bennett, B. D., Babu-Khan, S., Kahn, S., Mendiaz, E. A., Denis, P., Teplow, D. B., Ross, S., Amarante, P., Loeloff, R., Luo, Y., Fisher, S., Fuller, J., Edenson, S., Lile, J., Jarosinski, M. A., Biere, A. L., Curran, E., Burgess, T., Louis, J. C., Collins, F., Treanor, J., Rogers, G., and Citron, M. (1999) *Science 286*, 735−741.
8. Yan, R., Bienkowski, M. J., Shuck, M. E., Miao, H., Tory, M. C., Pauley, A. M., Brashier, J. R., Stratman, N. C., Mathews, W. R., Buhl, A. E., Carter, D. B., Tomasselli, A. G., Parodi, L. A., Heinrikson, R. L., and Gurney, M. E. (1999) *Nature 402*, 533−537.
9. Sinha, S., Anderson, J. P., Barbour, R., Basi, G. S., Caccavello, R., Davis, D., Doan, M., Dovey, H. F., Frigon, N., Hong, J., Jacobson-Croak, K., Jewett, N., Keim, P., Knops, J., Lieberburg, I., Power, M., Tan, H., Tatsuno, G., Tung, J., Schenk, D., Seubert, P., Suomensaari, S. M., Wang, S., Walker, D., John, V., et al. (1999) *Nature 402*, 537−540.
10. Hussain, J., Powell, D., Howlett, D. R., Tew, D. G., Meek, T. D., Chapman, C., Gloger, I. S., Murphy, K. E., Southan, C. D., Ryan, D. M., Smith, T. S., Simmons, D. L., Walsh, F. S., Dingwall, C. and Christie, G. (1999) *Mol. Cell. Neurosci. 14*, 419−427.
11. Tang, J., and Wong, R. N. (1987) *J. Cell. Biochem. 33*, 53−63.
12. Steiner, D. F. (1998) *Curr. Opin. Chem. Biol. 2*, 31−39.
13. Seidah, N. G., and Chretien, M. (1997) *Curr. Opin. Biotechnol. 8*, 602−607.
14. Ghosh, A., Shin, D., Downs, D., Koelsch, G., Lin, X., Ermolieff, J., and Tang, J. (2000) *J. Am. Chem. Soc. 122*, 3522−3523.
15. Leatherbarrow, R. J. (1998) Grafit version 4.0, Staines, U.K.
16. Bieth, J. (1994) *Bayer-Symposium V: Proteinase Inhibitors*, pp 463−469, Springer-Verlag, Berlin.
17. Latt, S. A., Auld, D. S., and Vallee, B. L. (1972) *Anal. Biochem 50*, 56−62.
18. Carmel, A., Zur, M., Yaron, A., and Katchalski, E. (1973) *FEBS Lett. 30*, 11−14.
19. Marciniszyn, J., Jr., Hartsuck, J. A., and Tang, J. (1976) *J. Biol. Chem. 251*, 7088−7094.
20. James, M. N., and Sielecki, A. R. (1986) *Nature 319*, 33−38.
21. Hartsuck, J. A., Koelsch, G., and Remington, S. J. (1992) *Proteins: Struct., Funct., Genet. 13*, 1−25.
22. Moore, S. A., Sielecki, A. R., Chernaia, M. M., Tarasova, N. I., and James, M. N. (1995) *J. Mol. Biol. 247*, 466−485.
23. Khan, A. R., Cherney, M. M., Tarasova, N. I., and James, M. N. (1997) *Nat. Struct. Biol. 4*, 1010−1015.
24. Heinrikson, R. L., Hui, J., Zurcher-Neely, H., and Poorman, R. A. (1989) *Am. J. Hypertens. 2*, 367−380.
25. Capell, A., Steiner, H., Willem., M., Kaiser, H., Meyer, C., Walter, J., Lammich, S., Multhaup, G., and Haass, C. (2000) *J. Biol. Chem.* (in press, published online ahead of print).

BI001494F